11th International Workshop on Computational Electronics
TU Wien, 25-27 May 2006

Physical Modeling of Electron Mobility Enhancement for Arbitrarily Strained Silicon

E. Ungersboeck, S. Dhar, G. Karlowatz, H. Kosina, and S. Selberherr
Institute for Microelectronics, TU Wien, Gußhausstraße 27–29/E360, 1040 Wien, Austria
e-mail: ungersboeck@iue.tuwien.ac.at

ABSTRACT

The band structure (BS) of Si with arbitrary stress/strain conditions has been calculated using the empirical non-local pseudopotential method (EPM). It is shown that the change of the effective masses cannot be neglected for general stress conditions and how this effect together with the strain induced splitting of the conduction bands can be used to optimize electron mobility enhancement $\Delta\mu_{\mathrm{n}}$. The new findings have been incorporated into an existing low-field mobility model.

BAND STRUCTURE CALCULATIONS

Strain effects on the electronic BS of Si are often described using deformation potential theory, which allows the determination of the strain induced splitting of the conduction bands. However, experiments [1] have shown that the mobility enhancement $\Delta\mu_{\mathrm{n}}$ cannot solely be attributed to this effect, and a recent study has shown that a stress along the $\langle 110\rangle$ direction leads to a change of the effective mass Δm^* [2].

In this work, the effect of general strain conditions on the BS is studied by means of EPM calculations. The number of symmetry elements $P(\Gamma)$ at the center of the Brillouin zone of the strained lattice determines the volume of the irreducible wedge via $\Omega_{\mathrm{irred}} = \Omega_{\mathrm{BZ}}/P(\Gamma)$. For stress along $\langle 100\rangle, \langle 111\rangle$, and $\langle 110\rangle$, as shown in Fig. 1, $P(\Gamma)$ is 16, 12, and 8, respectively, while for stress along other directions the lattice is invariant only to inversion, thus $P(\Gamma) = 2$.

MOBILITY ENHANCEMENT

Bulk mobility was calculated by means of Monte Carlo simulations [3]. In Fig. 2 the strain induced valley splitting is shown for biaxially strained and uniaxially stressed Si (along $\langle 110\rangle$ and $\langle 120\rangle$). It can be seen that biaxial tension is more effective in splitting the conduction bands than uniaxial tension in $\langle 110\rangle$ and $\langle 120\rangle$. Note that for $\langle 120\rangle$ stress the conduction bands split into three two-fold degenerate pairs. The in-plane effective masses of the lowest valley were extracted from EPM calculations. Fig. 3 shows how uniaxial tensile stress along $\langle 110\rangle$ yields a pronounced Δm_t, whereas the effect is smaller for stress along $\langle 120\rangle$ stress and negligible for biaxial tensile strain. The direction of stress in turn leads to a pronounced anisotropy of the mobility in the transport plane. In Fig. 4 the anisotropy of $\Delta\mu_{\mathrm{n}}$ is compared for different stress directions. It can be clearly seen that Δm_t cannot be neglected for $\langle 110\rangle$ uniaxial stress.

The two beneficial effects on the mobility arising from Δm_t and the valley splitting can be combined to yield the highest mobility enhancement in a system with in plane biaxial tension and uniaxial stress along $\langle 110\rangle$. In Fig. 5 the in-plane mobilities parallel and perpendicular to $[110]$ are shown.

The physically based low-field mobility model in [4] was extended to take into account the stress induced effective mass change of the lowest Δ_2 valley. For $\langle 110\rangle$ stress the effective mass tensor becomes non-diagonal, with $m_c/2(m_{t,\|}^{-1} + m_{t,\perp}^{-1})$ in the diagonal and $m_c/2(m_{t,\|}^{-1} - m_{t,\perp}^{-1})$ in the off-diagonal. Good agreement between Monte Carlo simulation and the analytical model is observed (Fig. 5).

This work has been partly supported by the Austrian Science Fund (FWF), project 17285-N02.

REFERENCES

[1] K. Uchida et al., IEDM, pp. 229–232 (2004).
[2] K. Uchida et al., IEDM, pp. 135–138 (2005).
[3] Institute for Microelectronics, VMC 1.0 User's Guide, TU Wien, http://www.iue.tuwien.ac.at/software/vmc (2004).
[4] S. Dhar et al., TED, vol. 52, pp. 527–533 (2005).

ISBN 3-901578-16-1

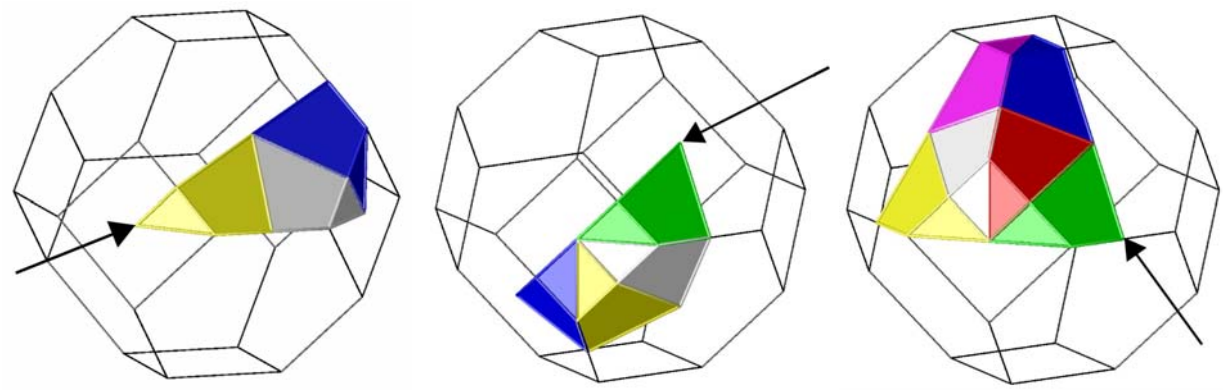

Fig. 1. Irreducible wedge for stress applied in [100], [111], and [110] direction.

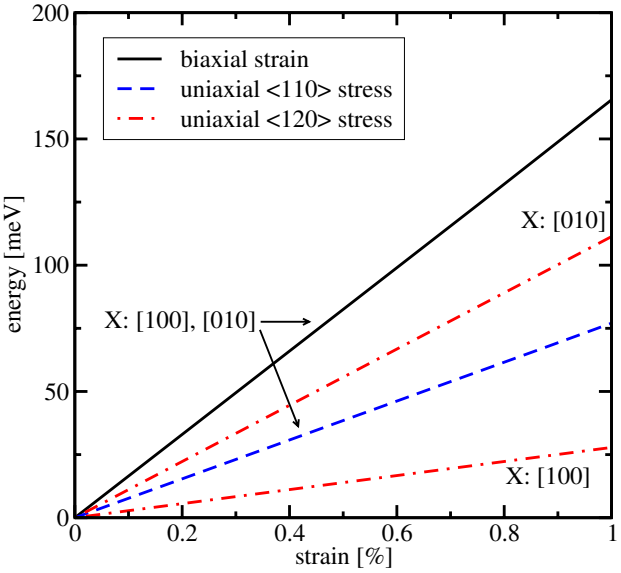

Fig. 2. Effect of biaxial tensile strain and uniaxial ⟨110⟩ and ⟨120⟩ tensile stress on valley splitting. Strain component in the stressed direction is plotted.

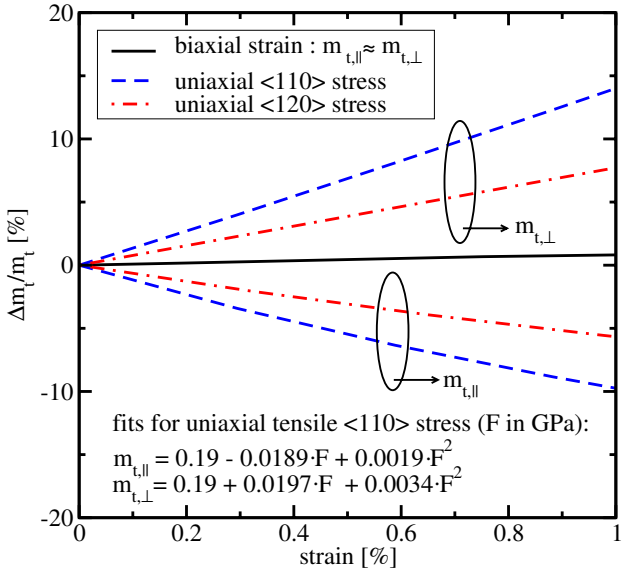

Fig. 3. Effect of biaxial tensile strain and uniaxial ⟨110⟩ and ⟨120⟩ tensile stress on the in-plane masses of the lowest valley.

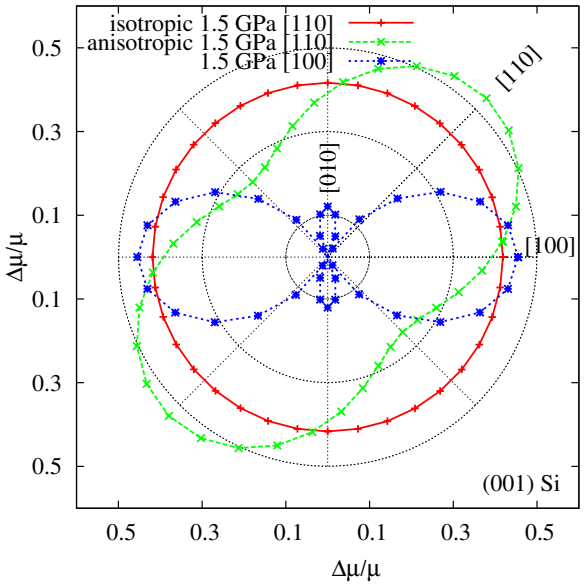

Fig. 4. Mobility enhancement for uniaxial ⟨110⟩ tensile and ⟨001⟩ compressive stress (equivalent to biaxial in-plane strain). The red line shows $\Delta\mu_n$ without the mass corrections.

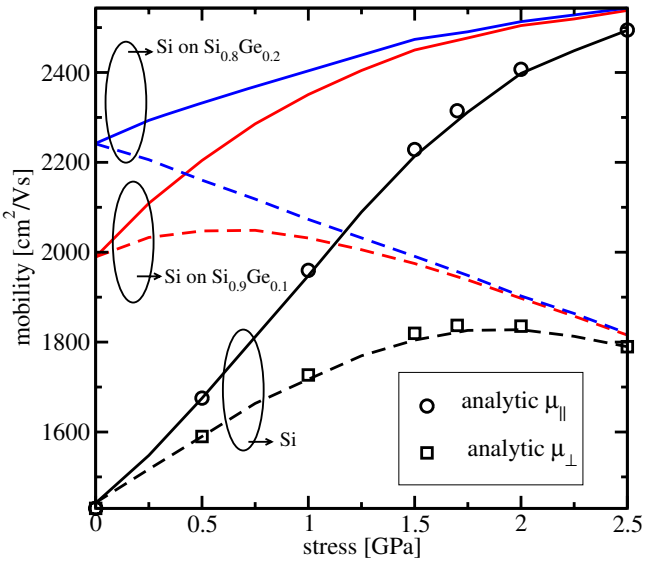

Fig. 5. Simulated bulk mobility for systems combing uniaxial ⟨110⟩ tensile stress and biaxial tensile strain in [110] (solid lines) and [$\bar{1}$10] (dashed lines) direction. The symbols show the mobility calculated from the analytic mobility model [4].